ClearSky: Satellite Imagery Based Deep Learning Model to Predict Wildfire Spread

Ahmet Ş. Yener Deniz Zağlı

Abstract

As wildfires rage across the entire continent of Australia, the lack of resources are more apparent than ever. When there are limited resources the lack of forecasts make the distribution of resources inefficient. This inefficiency has a wide range of effects, from human and animal life loses to monetary damage. Current in use forecast systems require expert knowledge to run and are case to case basis so the data available is not leveraged to the extent it should. We've developed a system that alleviates these problems combining GIS (Geographic Information Systems) and Deep Learning models that are used in meaning extraction from visual data. We've expanded and showed the agnosticism of the model to spatial,temporal data and underlying code frameworks. We propose future work that will increase efficiency and automate the system, making it distributable to the authorities around the globe.

1. Introduction

The current climate change effects create much more suitable conditions for wildfire outbreaks and spread (Clarke, Hamish, et al. (2019)). Wildfires across the globe are expected to rise in amount and intensity (Running, Steven W.,James, Sagil, et al. "Smart Drone Technology for Wildfire Prediction and Prevention." (2019)., (Chung, M., M. Jung, and Y. Kim. et al. (2019).) While detection is possible, forecast on the spread of the wildfire is a critical information for minimizing the damage caused.

Data we are using is widely spread and do not exist in an analyzable form in any single place. This obscurity by diffusion limits the amount of work done on such a critical area. Data in it's provided form needs heavy processing and geo-referencing to be able to analyzed by the Deep Learning models. These obstacles can be automated with collaboration by the data providers. The upside is that the datasets used are all publicly available.

We use Satellite generated imagery combined with GIS applications to generate input and create ground-truth for the supervised Deep Learning model. The prediction ability of the Deep Learning model combined with GIS applications to provide spatial characteristics such as elevation, health and the density of vegetation at that area proves to be able to forecast the highly chaotic event which are wildfires.

Entire system after processing can be run on mid level machines, and operating systems supporting the libraries used. The prediction is of highly interpretable form without prior training on the legend, combined with low computational and memory costs make the model appropriate for field use. We hope the system in use can reduce all types of damages to human, animal life and will provide a livable future for the children of humanity. We contribute in this paper proof of agnosticism to the spatial and temporal characteristics of the wildfire to the system proposed in the FireCast paper (Radke, David, Anna Hessler, and Dan Ellsworth. "Firecast: leveraging deep learning to predict wildfire spread." Proceedings of the 28th International Joint Conference on Artificial Intelligence . AAAI Press, 2019.) and some further data and model complexity reduction.

2. Related Work

The first of it's kind the Deep Learning Model proposed by the above cited paper has been a major inspiration for this paper. Their model presented in the paper is implemented with PyTorch and the dataset providers proposed by them are used in our own compiled dataset.

Their work was done on the Rocky Mountain range with limited availability of consecutively mapped perimeter for the day, We have gathered our data from the entire area of the state of California. The wildfire outbreak of 2018 provides a great amount of data, combined with 2017 data to prove robustness against changing conditions of the outbreak locations and time.

Since the data is unique in its relation to the fire only rotation is suitable as an augmentation. This means the current methods in use that provide expansion of the dataset to the model are not suitable for this task, so the amount of original data is highly valuable for the prediction capability of the model.

3. The Approach

3.1. Input

The predictive data to model fire behaviour represents a triangle (Figure 1).

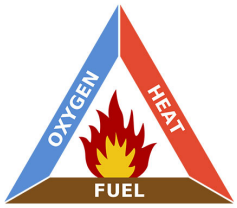

Figure 1. Fire Triangle

Fuel which is the vegetation subjected to burn; Geographical information of the area such as elevation,aspect and slope; Weather information of the area such as dew point, temperature, wind direction and speed constitute the sides of this triangle. (Quintiere, James G. Principles of fire behavior . CRC Press, et al. 2016.) We have extracted from dataset's below and processed them to have a machine readable form for the information needed to predict fire behaviour.

One of the data we use in the input is Landsat 8 satellite data. Landsat images are provided with resolution of 30m x 30m and generally taken with 16 day intervals between same location imaging. We extract the landsat image closest to the fire outbreak with as minimal cloud cover as possible (range 0,20 percent cloud cover). Since the health of vegetation is not highly changing we believe there is minimal information loss from a landsat data extracted just the day before the wildfire outbreak.

We accessed Landsat 8 satellite data via GloVis, which was launched by the US Government. NASA produces this data. We used Band 2 (Blue) (Figure 2), Band 3 (Green) (Figure 3), Band 4 (Red) (Figure 4) and Band 5 (Near Infrared) (Figure 5).

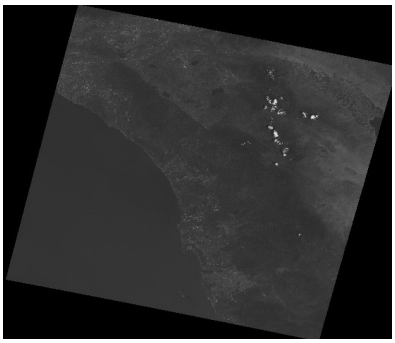

Figure 2. Band 2 (Blue)

The other satellite data we need is NDVI (Normalize Difference Vegetaion Index) (Figure 6). We cannot access this data via GloVis. So we have to calculate ourselves.

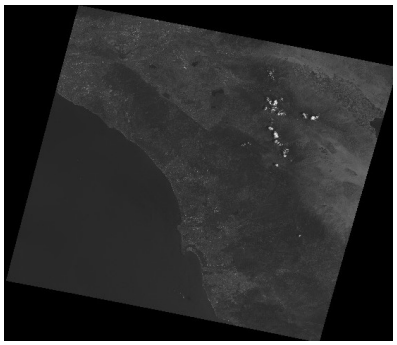

Figure 3. Band 3 (Green)

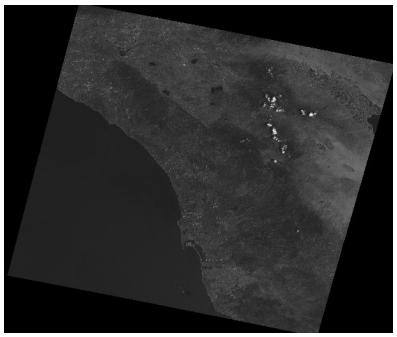

Figure 4. Band 4 (Red)

Digital elevation model is provided to provide geographical information of that point. DEM supports processing for aspect (Figure 8) and slope (Figure 9) for the area which we believe provides enough geographical information for the spread of the fire at that area. We accessed DEM data thanks to the WCS Server connection made available by the U.S. Government.

Another input is Weather data (Figure 10). The relevant weather data is extracted from NOAA HRRV1 archive with (3km x 3km) spatial resolution. We sample the weather data a single time as close to the fire growth border as possible but a more precise data gathering should be done to increase accuracy of the forecast.

Another input is fire data. We used GeoMAC's fire data for this data. This fire data is a Shape File. We created the starting-perimeter (Figure 11) and ending-perimeter (Figure 12) by augmenting the Shape file on Landsat-8 satellite data.

3.2. Data Processing

We used the raster calculator of Qgis to do this calculation. After collecting the desired Landsat 8 satellite data, we started to combine this data with the fire perimeter. We

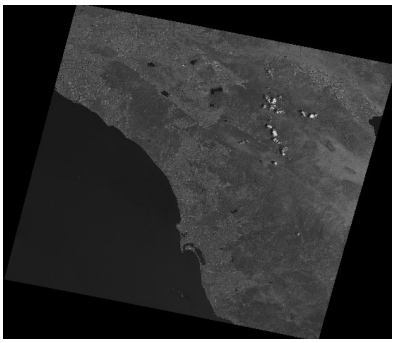

Figure 5. Band 5 (Near Infrared)

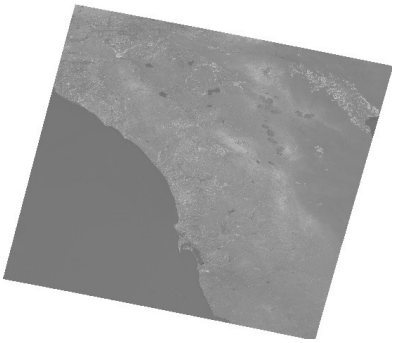

Figure 6. NDVI(Normalized Difference Vegetation Index)

performed this merge to create a fire and non-fire map. We have explained this merging process and how we create the starting-perimeter (Figure 11) and ending-perimeter (Figure 12) map as a result of this merging on Qgis:

- Filter GeoMAC data in Shape File format according to a single fire of your choice.

- Save this fire as you filter.

- Open the Landsat-8 data in TIFF format.

- Open this fire data, which is the only one you have saved.

- By applying Qgis clip process, we will clip our raster data according to the shape file boundaries. As a result of this clip, we will have a rasterized clip.

- As a final process, we will create our starting-perimeter (Figure 11) and ending-peirmeter (Figure 12) map by applying Qgis's AND operation between this raster and Landsat-8 satellite data.

The projections must be the same if we want to process between the Shape File and the TIFF File. In this project we used EPSG: 4269 as a projection. After creating the starting-perimeter, we used only the pixels outside the fire to make more efficient use of the data we hold. For this we have created a dilated border (Figure 13).

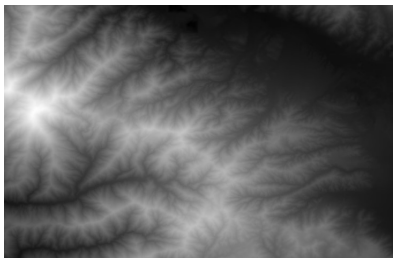

Figure 7. 3DEP (3D Elevation Program)

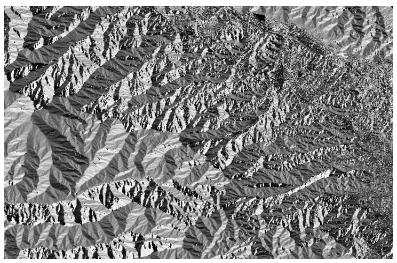

Figure 8. Aspect Degree

We used WCS Server connection over QGis for DEM data. Since this data is too large, we need to clip it carefully. We have described the following clipping process and how to make the data available:

- First of all, we save the largest version of the data as Shape File. The reason for this is that there is no loss of pixels when we examine a larger fire.

- Then, with this Shape File, we need to apply raster extraction from Landsat-8 satellite data of that data. We've explained this above.

- We will get the map we want with this cut raster. For this, we cut this raster separately for 3DEP, Aspect Degree, Slope Degree by showing the mask. Since we want the result of this cutting in TIFF format, we do this by selecting tiff in the select format section of the save as option.

- After obtaining the cut raster, we have to place it on the Landsat-8 satellite data and in Qgis we apply the following raster calculation: "TIFF + (LANDSAT AND 0)". In this way, we create a TIFF file that has Landsat-8 satellite data size but only data at the desired location.

We used raster calculation via Qgis to obtain NDVI (Figure 6) data. We obtained NDVI (Figure 6) data using Band 4 (Red) and Band 5 (NIR). The formula required for this is shown below:

$$NDVI = \frac{BAND5(NIR) - BAND4(RED)}{BAND5(NIR) + BAND4(RED)}$$

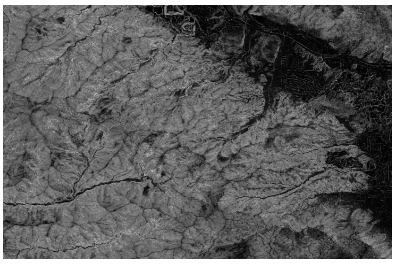

Figure 9. Slope Degree

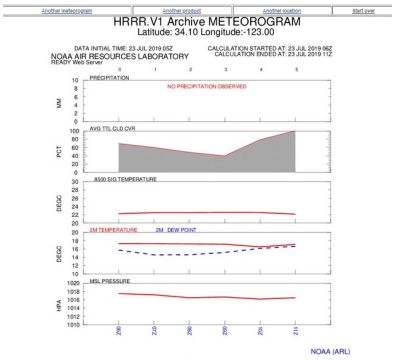

Figure 10. NOAA

Figure 11. Starting-Perimeter

Figure 12. Ending-Perimeter

3.3. Algorithm

Extraction of generalizable knowledge suited for forecasting from data has been done by CNN's on a wide variety of tasks to state of the art accuracies. (Aimal, Syeda, et al. 2019.) (Tran, Trung-Tin, et al. (2019)). Chaotic system forecasting has been done by combining CNN's with LSTM's while we do not implement this system right now it shows a way for future work with better accuracies (Chen, Rui, et al (2019))

We implement a 2D CNN detailed in the figure (Figure 14)below:

We dilate the starting-perimeter (Figure 11) with a predetermined dilation size which is a hyper-parameter. Subtracting the starting-perimeter (Figure 11) from this dilated image (Figure 13) leaves us with list of vulnerable pixels for the next day. We sample these points and balance them in two ways:

The sampled points for a single day must contain equal amounts of burned and not burned pixels from the next day perimeter. This approach should provide robustness against under or over prediction of burning pixels relative to not burned pixels.

The sampled points from a single burn must not dominate the dataset relative to its size. Omitting this biases the training data to bigger fires. This approach should provide robustness to differing fire sizes.

A 60 x 60 image patch is extracted from the combined spatial data and then subjected to convolution operations intersped with pooling operations. The activation function is sigmoid for all of the layers for we are looking at predictions on the range [0,1]. Ground-truth for the supervised learning is the burn condition in the next day perimeter (Table 1) as such:

0	1
not burn	burn

Table 1.

The final output of the convolutional layer is then flattened, concatenated with the weather data Connected to a single output neuron, the sigmoid squished the information between [0,1] Loss is calculated as binary-cross entropy from the value of the output neuron and then back propagated across the system.

We imbue meaning to the output (Table 2) as such:

less than 0.5	greater or equal than 0.5
not burn	burn

Table 2.

Validation is done on fires omitted from the dataset. They

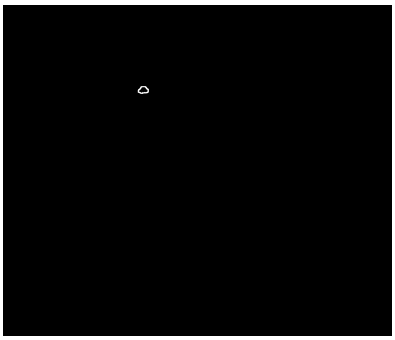

Figure 13. Dilated Border

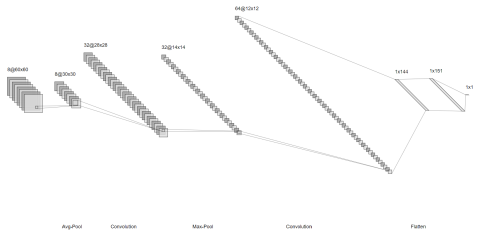

Figure 14. Architecture

are sampled completely randomly with denser sampling for closer to true 2D output.

4. Experimental Results

Our Prediction	Real	Colour
burn	burn	Red
burn	not burn	Black
not burn	burn	White
not burn	not burn	Blue

Table 3.

4.1. Statistical Evaluation of the Model

$$Precision = \frac{tp}{tp + fp}$$

$$Recall = \frac{tp}{tp + fn}$$

$$F = 2 * \frac{precision * recall}{precision + recall}$$

We have used the above formulas to calculate the model's success on detecting fire, which is statistically significant.

Figure 15. Field with wildfire

Figure 16. GeoMAC data of forest fire

We report an average F score of 10.18 percent on 6 test fires, 3 of them belonging to the same burn-mass with following day couples and the other 3 each a burn instance on its own regard.

Figure 17. Day 1 of the wildfire

4.2. Day 1 Predictions

4.2.1. Wrong Prediction of Danger

The lower border of the fire is deemed to be in no danger of fire spread while there is a spread observed in Day 2 (Figure 18).This can be infered from the legend as it is nearly completely black (non predicted actual burn signifier). It is interesting that the spread stops after burning a small amount of area Day 2 (Figure 18) and no further spread is detected on Day 3 (Figure 19), How does this information relates to the prediction on Day 3 (Figure 19) should be further analyzed.

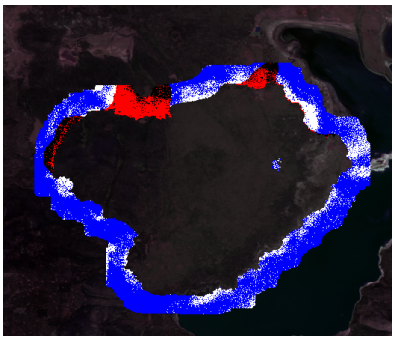

Figure 18. Day 2 of the wildfire

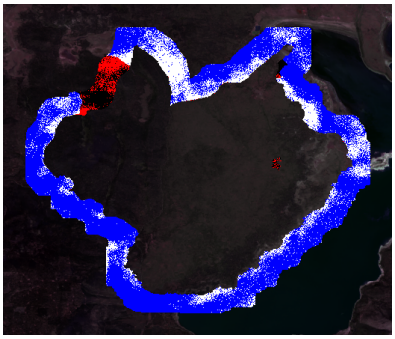

Figure 19. Day 3 of the wildfire

4.2.2. Right prediction of non-danger

The left side of the fire features a sparse forest population residing on a steep mountain hill where the fire has no spread vector present, this information is learned correctly by the machine and represented by mostly solid blue border.

4.2.3. Right prediction of danger

The heavy red dotted area featured on the upper and right side of the fire indicates a high danger of spread to that area. There is an observed spread in a huge amount there, the main spread vector of the fire can be predicted on day 1 (Figure 17), which proves the model output given to fire fighting crews on the field on day 1 (Figure 17) could be used to effectively stop the massive burn observed on Day 2 (Figure 18).

4.3. Day 2 Predictions

4.3.1. Wrong Prediction of Danger

Where there are featured white spots, a spread is predicted where there is none. It is observed That these white spots are featured not touching the border, meaning a spread is predicted which will stop that day without breaking the danger zone.

4.3.2. Right prediction of danger

When the prediction of fire touches the border that means an imminent spread danger is predicted where the resources should be used to stop the spread there. The huge spike shaped spreads in these days are correctly predicted with red-to-the-border visual output of the fire

5. Limitations

Since fires when detected are subject to fire-fighting by the authorities the data acquired does not have information about it which effects the growth of the fire nearly as much as the other variables presented. The satellite based nature of the data is obscured by the smoke emitted by the fire which lovers the accuracy of observations for this task.

6. Future Work

There is a ceiling to the amount of data gatherable by the datasets in use. Since the perimeter data is drawn or satellite detected there exist a lot of noise from the actual observed fire. The small amount of data available and the lack of automation these systems lends itself to opens up a lot of directions for improvement on both dataset aspect and model's ability to deal with expected forecasting task.

7. Improvements

7.1. Dataset Improvements

The MODIS FIRE PRODUCT (Giglio, Louis, Wilfrid Schroeder, and Christopher O. Justice. et. al.(2016)) available from servers of the University of Maryland comes with both upsides and downsides for the task.

It has consecutive mappings of observed fires in 12 hour temporal resolution since 2015. It also comes with QA bits associated with observed fires signifying the confidence of pixel being on fire. It's spatial resolution is 1km x 1km which is lower than the dataset we are using.

While the spatial resolution is much lower; combination of the much higher amount of data, data noise expectation and the higher temporal resolution will provide a better forecasting ability.

7.2. Model Improvements

The time series nature of the data is foregone with the current in use model which is a cnn capable of training only on perimeter couples. The output of the model is pseudo-2D which means there are missing points which may prove vital to the forecasting ability. The type of 2D output expected of the machine is much more suitable to Auto-Encoders such as UNet used in (Jin, Qiangguo, et al. (2018)). The time series

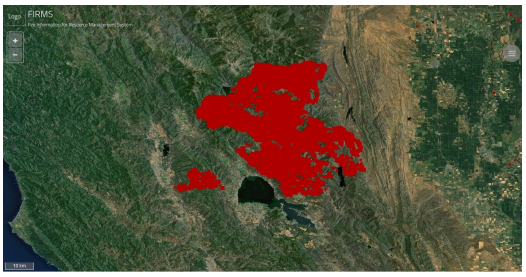

Figure 20. MODIS Data

nature of the forecasting combined with the expected output type seems to lends itself much more to models capable of analyzing spatio-temporal data proposed in.

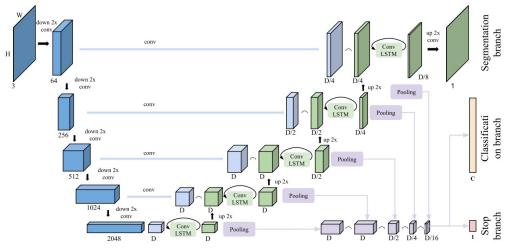

Figure 21. UNET LSTM

References

Stephens et al., 2018] Scott L. Stephens, Brandon M. Collins, Christopher J. Fettig, Mark A. Finney, Chad M. Hoffman, Eric E. Knapp, Malcolm P. North, High Safford, and Rebecca B. Wayman. Drought, tree mortality, and wildfire in forests adapted to frequent fire. BioScience, 68(2):77–88, Feb 2018.

Clarke, Hamish, et al. "Climate change effects on the frequency, seasonality and interannual variability of suitable prescribed burning weather conditions in south-eastern Australia." Agricultural and Forest Meteorology 271 (2019): 148-157

Running, Steven W. "Is global warming causing more, larger wildfires?." Science 313.5789 (2006): 927-928.

James, Sagil, et al. "Smart Drone Technology for Wildfire Prediction and Prevention." (2019)., (Chung, M., M. Jung, and Y. Kim. "WILDFIRE DAMAGE ASSESSMENT USING MULTI-TEMPORAL SENTINEL-2 DATA." International Archives of the Photogrammetry, Remote Sensing Spatial Information Sciences (2019)

Radke, David, Anna Hessler, and Dan Ellsworth. "Firecast: leveraging deep learning to predict wildfire spread." Proceedings of the 28th International Joint Conference on Artificial Intelligence . AAAI Press, 2019

Quintiere, James G. Principles of fire behavior . CRC Press, 2016

Robinson, Nathaniel, et al. "A dynamic Landsat derived normalized difference vegetation index (NDVI) product for the conterminous United States." Remote Sensing 9.8 (2017): 863

Aimal, Syeda, et al. "An Efficient CNN and KNN Data Analytics for Electricity Load Forecasting in the Smart Grid." Workshops of the International Conference on Advanced Information Networking and Applications . Springer, Cham, 2019.

Tran, Trung-Tin, et al. "A Comparative Study of Deep CNN in Forecasting and Classifying the Macronutrient Deficiencies on Development of Tomato Plant." Applied Sciences 9.8 (2019): 1601

Chen, Rui, et al. "A hybrid CNN-LSTM model for typhoon formation forecasting." GeoInformatica (2019): 1-22

Giglio, Louis, Wilfrid Schroeder, and Christopher O. Justice. "The collection 6 MODIS active fire detection algorithm and fire products." Remote Sensing of Environment 178 (2016): 31-41

Jin, Qiangguo, et al. "RA-UNet: A hybrid deep attention-aware network to extract liver and tumor in CT scans." arXiv preprint arXiv:1811.01328 (2018)

Yu, Bing, Haoteng Yin, and Zhanxing Zhu. "ST-UNet: A Spatio-Temporal U-Network for Graph-structured Time Series Modeling." arXiv preprint arXiv:1903.05631 (2019)

Arbelle, Assaf, and Tammy Riklin Raviv. "Microscopy cell segmentation via convolutional LSTM networks." 2019 IEEE 16th International Symposium on Biomedical Imaging (ISBI 2019) . IEEE, 2019

https://glovis.usgs.gov/

https://www.ready.noaa.gov/READYamet.php

https://elevation.nationalmap.gov/arcgis/rest/services/3DEPElevation/ImageServer